

Far-infrared response of lateral superlattices in high magnetic fields

Axel Lorke,* Igor Ješina, and Jörg P. Kotthaus

Sektion Physik, Universität München, Geschwister-Scholl-Platz 1, 8000 München 22, Germany

(Received 14 July 1992; revised manuscript received 31 August 1992)

We study the high-frequency response of lateral superlattices in high magnetic fields in the transition regime from a two-dimensional electron gas to isolated electron dots. For largely different samples we find that the far-infrared-active modes of electron dots and antidots develop out of the cyclotron resonance rather than out of the magnetoplasmon. The transition from the (single) cyclotron resonance to the two resonances that make up the antidot spectrum takes place quite abruptly when the potential maxima start to exceed the Fermi energy. A classical, single-particle model of ballistically moving electrons is presented that can account for the experimental observations. In view of these findings the role of many-particle contributions in lateral superlattices in high magnetic fields is discussed.

It is now understood that the dynamic response of typical mesoscopic electron systems on semiconductors, such as quantum wires and quantum dots,¹ can be well described assuming a parabolic confining potential. The dominant far-infrared modes then reflect the collective center of mass motion of all electrons in the bare confining potential.^{2,3} Therefore, the high-frequency magnetotransport properties of such systems can be calculated with relative ease in either a classical⁴ or a quantum-mechanical^{5,6} single-particle picture or in a many-particle picture of excitations of a confined plasma.⁷ All these approaches lead to qualitatively identical results for the magnetic-field dispersion and it is difficult to estimate from the experiments which effects dominate the observed resonance positions.⁸

Recently, more complicated structures, such as coupled dots⁹ and antidots,^{10,11} have been investigated where no simple analytical models are at hand to describe the experimental observations. The purpose of this paper is to investigate experimentally as well as through numerical simulations the high-magnetic-field dynamic response of lateral superlattices, ranging from the well-understood case of a two-dimensional electron gas (2DEG) over antidots to the (again well-understood) case of isolated dots.

The experiments have been carried out on two different kinds of samples: a GaAs quantum-well structure with a corrugated gate and a Si metal-oxide-semiconductor structure with a stacked gate. The preparation of such samples is described in detail elsewhere.^{9,12,13} In both samples a patterned gate with square symmetry enables us to impose a periodic potential upon the electron gas that can be finely tuned *in situ* by changing the applied gate voltage.

Figures 1(a)–1(c) display different situations that can be achieved by changing the amplitude of the superlattice potential relative to the Fermi energy. Figure 1(a) corresponds to a weakly modulated 2DEG, Fig. 1(b) to an array of antidots, and Fig. 1(c) to the situation of isolated dots. Figure 1(d) displays a capacitance-voltage trace of the GaAs sample with a period $a = 460$ nm. At low negative gate voltages ($-V_g \leq 1.5$ V) the modulation amplitude is still low [Fig. 1(a)] and the capacitance is at its

maximum. At $-V_g \approx 1.7$ V the capacitance abruptly drops as parts of the sample become depleted and antidots develop [Fig. 1(b)]. At voltages above 2.7 V the capacitance drops dramatically as the pattern transforms into an array of isolated dots and the signal is governed by the poorly conducting back contact layer.⁹

The dynamic response of the samples in magnetic fields applied perpendicularly to the lateral superlattice is studied at liquid-He temperatures in the range between 15 and 100 cm^{-1} using a Fourier transform spectrometer. Figure 2(a) shows the experimental resonance positions of the GaAs sample at a fixed magnetic field $B = 3$ T as a function of gate voltage. It can be seen that the modes develop in correlation to the modulation patterns as derived from the capacitance trace. At $-V_g = 0$ V, the electron system is a 2DEG with only little potential modulation and a cyclotron resonance at 40 cm^{-1} is observed as well as a magnetoplasmon at a wave vector $q = 2\pi/a$ at 73 cm^{-1} . Between $-V_g = 0$ and 1.5 V the cyclotron frequency ω_c is independent of the gate voltage, although at 1.5 V the electron gas is already strongly modulated. Between $-V_g = 1.5$ and 2.5 V, when the sample becomes partially depleted and antidots form, the

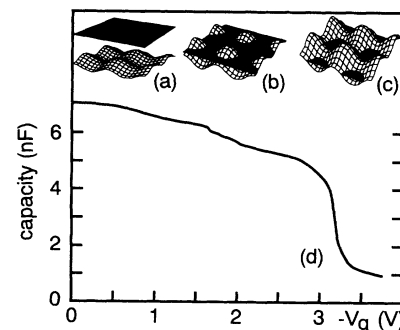


FIG. 1. (a)–(c) Schematic representation of different patterns that can be obtained using gate-voltage-controlled lateral superlattices: (a) weakly modulated 2DEG, (b) antidots, (c) dots. The Fermi energy is indicated in black. (d) Capacitance-voltage trace of the GaAs sample at $T = 2$ K.

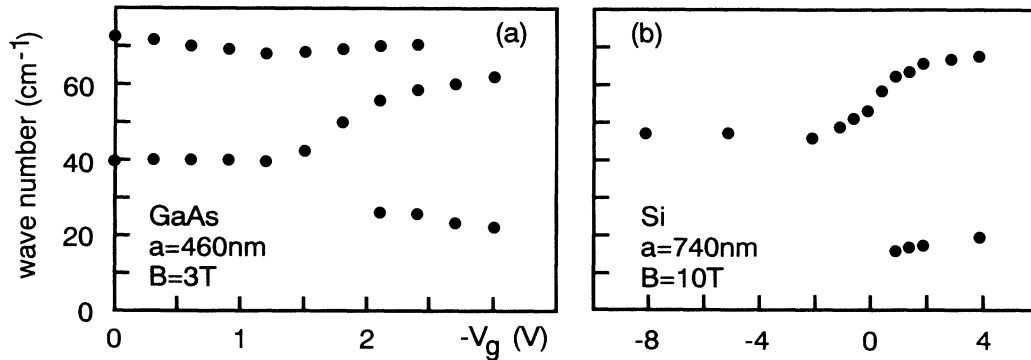


FIG. 2. Measured far-infrared resonance frequencies as a function of gate voltage for (a) the GaAs and (b) the Si sample. In (b) the voltage of the second (top) gate, which essentially controls the carrier density, is kept at $V_{gt} = 18$ V (cf. Refs. 12 and 13).

cyclotron frequency ω_c is independent of the gate voltage, although at 1.5 V the electron gas is already strongly modulated. Between $-V_g = 1.5$ and 2.5 V, when the sample becomes partially depleted and antidots form, the cyclotron mode dramatically shifts upwards and a second resonance appears at frequencies below ω_c . When the narrow constrictions between the antidots become depleted around $-V_g = 2.7$ V, the magnetoplasmon, which is essentially a two-dimensional excitation, dies out and the characteristic two-mode spectrum of parabolically confined dots establishes. In this regime an additional mode reflecting a molecular orbit has been observed⁹ which lies too low in frequency to be unambiguously identified in this experiment.

Figure 2(b) displays the resonance positions of the Si sample. Although this sample is different in material, gate pattern, and period, the overall development of the observed resonances is the same as in the GaAs sample at sufficiently high magnetic fields. The magnetoplasmon, which is expected around 65 cm^{-1} , cannot be unambiguously identified in the Si sample at magnetic fields above 8 T where it starts to merge with the cyclotron resonance.

At low fields, where the cyclotron frequency is much smaller than the characteristic frequency of the confining potential of the dots, the development of the upper-dot mode out of the cyclotron resonance is not as clear in either sample. In this low-field regime the magnetic length scale is of the order of the lattice constant and an intriguing energy spectrum has been calculated in a quantum-mechanical approach by Hofstadter.¹⁴ However, in the present sample, where Hofstadter's assumption of low electric and magnetic quantum numbers is not fulfilled, a picture of *classical*, chaotic motion¹⁵ is more appropriate. In the following we will restrict ourselves to the case of high magnetic fields.

As mentioned above, both limits of an unmodulated 2DEG and isolated dots can be qualitatively described in a simple, single-particle picture.^{4-6,16} In the following, we will extend this picture to the intermediate regime, using a technique that has successfully been employed in modeling the low-frequency transport properties of lateral superlattices^{17,15} and the magnetic-field dispersion of the

high-frequency modes in antidots.¹⁸

To obtain the far-infrared-active modes of lateral superlattices we calculate the ballistic trajectories of a large set ($10^3 - 10^4$) of electrons in the lattice by numerically integrating the classical equation of motion. The required initial conditions are chosen at random such that the total energy of each electron corresponds to the Fermi energy in a typical experimental situation. The thus obtained trajectories are then evaluated for their eigenfrequencies. To test for a frequency ω the velocity component $v_x(t)$ of each trajectory i is multiplied by $\cos(\omega t)$ and integrated over the scattering time τ_i :

$$I_1(\tau_i) = \int_0^{\tau_i} v_x(t) \cos(\omega t) dt .$$

To compensate for the uncertainty in phase we also determine

$$I_2(\tau_i) = \int_0^{\tau_i} v_x(t) \sin(\omega t) dt$$

and obtain the superlattice response by averaging over all scattering times and initial conditions

$$I(\omega, \tau) = \langle \sqrt{I_1^2 + I_2^2} \rangle .$$

Here the scattering times τ_i are chosen at random such that the ensemble exponentially decays with a lifetime τ that accounts for mobilities found in high-quality samples. It can be shown that $I(\omega)$ properly reproduces any spectrum of v_x that consists of sufficiently high ($\omega\tau \gg 1$)

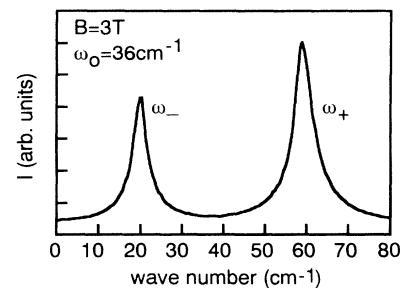


FIG. 3. Calculated far-infrared spectrum of parabolic electron dots in a magnetic field.

and well-separated ($\Delta\omega\tau \gg 1$) frequencies. The experimental far-infrared response of lateral superlattices which is governed by the real part of the high-frequency conductivity, can therefore directly be compared with the results of the simulation.

Figure 3 displays a calculated spectrum $I(\omega)$ at $B = 3$ T of electron dots on GaAs that are confined in a parabolic potential with a characteristic frequency $\omega_0 = 36 \text{ cm}^{-1}$. Two resonances, ω_+ and ω_- , can be observed. Their frequency as a function of ω_0 and B is in good agreement with the experiment and with the dispersion $\omega_{\pm} = \sqrt{\omega_0^2 + \omega_c^2}/4 \pm \omega_c/2$, derived analytically by Wilson, Allen, and Tsui.^{4,19} However, their *line shape*, namely, the fact that the ω_- mode exhibits a smaller amplitude than the ω_+ mode, whereas the width of both modes is equal, is in disagreement with the analytical model. The reason for this discrepancy is that the analytical model introduces a phenomenological friction term in the equation of motion. A friction term which is proportional to the velocity, however, is of little meaning especially for the ω_- mode which corresponds to the drift of the cyclotronlike orbit along the equipotential lines in the dot. The results of our calculations rather resemble the quantum-mechanical result that has been derived using the Kubo formalism.⁶

So far, we have taken the curvature of the parabolic potential from the experimentally observed resonance frequencies. According to the “generalized Kohn theorem”² this is the curvature of the *bare* potential which is provided by all external charges. Screening by the mobile electrons in the dot causes the curvature of the “real” (self-consistent) potential to be much smaller.¹ Therefore, for a given superlattice period a , one could only account for the experimentally observed frequencies by assuming unrealistically high potential amplitudes V_0 and Fermi energies (cf. Fig. 1). In the following we will rather use typical experimental values for a , E_F , and V_0 , and scale down the magnetic field to ensure $\omega_0 \approx \omega_c$ as in the experiments.

To model the entire transition regime from a 2DEG to electron dots, we calculate the trajectories of electrons in a two-dimensional periodic potential $V(x,y)$ under the influence of a magnetic field. For simplicity, only the lowest Fourier components of $V(x,y)$ were taken into account:

$$V(x,y) = \frac{V_0}{4} [\cos(kx) + \cos(ky) + 2], \quad k = 2\pi/a.$$

Figure 4 shows the result of the calculation for a magnetic field of $B = 0.6$ T, a period of $a = 450$ nm, a Fermi energy of $E_F = 17$ meV, and a potential modulation in the range of $0 < V_0 < 2.5E_F$. As long as $V_0 < E_F$, only one mode can be identified which exhibits the frequency of the cyclotron resonance. At $V_0 \approx E_F$, when the potential maxima start to exceed the Fermi energy and the antidots

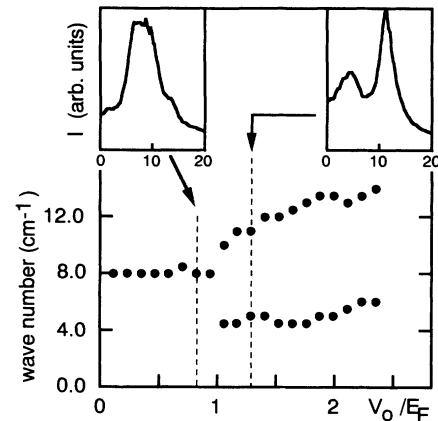


FIG. 4. Calculated resonance positions of a lateral superlattice as a function of potential modulation. The parameters used are $a = 450$ nm, $m^* = 0.07m_e$, $E_F = 17$ meV, to account for typical GaAs samples. A magnetic field of only 0.6 T was chosen for reasons discussed in the text. The insets display calculated spectra at $V_0 = 0.82^*E_F$ and 1.30^*E_F , respectively.

develop, the resonance quite abruptly splits into two. As the modulation becomes stronger, the splitting increases and finally approaches that of isolated dots. All these observations are in good qualitative agreement with the experimental data in Fig. 2. This result is remarkable, since it indicates that even for a fairly complicated potential modulation the single-particle approximation can be used. Similar to the case of parabolic confinement, the electron-electron interaction seems to only shift the energy scale.

In summary, we have experimentally investigated the development of the far-infrared-active modes of two-dimensional lateral superlattices in high magnetic fields. The observed development of the resonant modes as a function of the strength of the periodic potential has been compared with the results of a classical, single-particle model. The good qualitative agreement between the experiments and the calculations indicate that in high magnetic fields the electron-electron interaction merely shifts the energy scale of the experimentally observed dispersion. A rigorous proof of this observation has so far only been given for parabolically confined dots. Our findings extend that picture to the more general case of strongly modulated 2DEG's, antidots, and “nonparabolic” dots, giving it a wide applicability for the modeling of lateral superlattices and mesoscopic systems. However, a more complete picture that includes chaos¹⁵ as well as many-particle and quantum-mechanical effects is highly desirable for a deeper understanding of such structures.

We would like to thank T. Geisel for valuable discussions and acknowledge financial support by the ESPRIT Basic Research action.

*Present address: Materials Department, University of California, Santa Barbara, CA 93106.

¹For a recent review see, e.g., W. Hansen, J. P. Kotthaus, and U. Merkt, in *Semiconductors and Semimetals*, edited by R. K.

Willardson, A. C. Beer, and E. R. Weber (Academic, San Diego, 1992), Vol. 35, pp. 277–378.

²L. Brey, N. F. Johnson, and B. I. Halperin, *Phys. Rev. B* **40**, 10 647 (1989).

- ³P. A. Maksym and T. Chakraborty, *Phys. Rev. Lett.* **65**, 108 (1990).
- ⁴B. A. Wilson, S. J. Allen, Jr., and D. C. Tsui, *Phys. Rev. B* **24**, 5887 (1981).
- ⁵V. Fock, *Z. Phys.* **47**, 446 (1928).
- ⁶U. Merkt, Ch. Sikorski, and J. Alsmeier, in *Spectroscopy of Semiconductor Microstructures*, edited by G. Fasol, A. Fasolino, and P. Lugli (Plenum, New York, 1989), p. 89.
- ⁷S. J. Allen, Jr., H. L. Störmer, and J. C. M. Hwang, *Phys. Rev. B* **28**, 4875 (1983); A. L. Fetter, *ibid.* **33**, 5221 (1986).
- ⁸However, it has been shown that quantization of *charge* affects the integrated absorption strength. B. Meurer, D. Heitmann, and K. Ploog, *Phys. Rev. Lett.* **68**, 1371 (1992).
- ⁹A. Lorke, J. P. Kotthaus, and K. Ploog, *Phys. Rev. Lett.* **64**, 2559 (1990).
- ¹⁰A. Lorke, J. P. Kotthaus, and K. Ploog, *Superlatt. Microstruct.* **9**, 103 (1991).
- ¹¹K. Kern, D. Heitmann, P. Grambow, Y. H. Zhang, and K. Ploog, *Phys. Rev. Lett.* **66**, 1618 (1991).
- ¹²J. Alsmeier, E. Batke, and J. P. Kotthaus, *Phys. Rev. B* **41**, 1699 (1990).
- ¹³I. Jejina, H. Lorenz, J. P. Kotthaus, and S. Bakker (unpublished).
- ¹⁴D. R. Hofstadter, *Phys. Rev. B* **14**, 2239 (1976).
- ¹⁵R. Fleischmann, T. Geisel, and R. Ketzmerick, *Phys. Rev. Lett.* **68**, 1367 (1992).
- ¹⁶W. Kohn, *Phys. Rev.* **123**, 1242 (1961).
- ¹⁷A. Lorke, J. P. Kotthaus, and K. Ploog, *Phys. Rev. B* **44**, 3447 (1991).
- ¹⁸A. Lorke, *Surf. Sci.* **263**, 307 (1992).
- ¹⁹The calculated magnetic-field dispersion of slightly “nonparabolic” dots can be found in Ref. 18, as well as a comparison with the experiment and the analytical model.